Mathematical Modeling and Experimental Study of Conveyor Belt Continuous Curing Process

H. NAZOCKDAST, F. GOHARPEY, B. DABIR

Polymer Engineering Department, Amirkabir University of Technology, Tehran Iran

Received 14 March 1999; accepted 8 October 1999

ABSTRACT: A mathematical model was developed to predict the temperature distribution within various layers of conveyor belts during the continuous curing process. The results predicted by the model are found to be in good agreement with the experimental results, hence justifying the capability of the model for simulation of the conveyor belt continuous process. This information was utilized to provide more insight into the curing process in terms of the state of cure (SOC) and/or the degree of conversion, which may, in turn, be utilized for the optimization of the curing process. © 2000 John Wiley & Sons, Inc. J Appl Polym Sci 77: 2448–2454, 2000

Key words: conveyor belt; continuous curing; mathematical modeling; heat of vulcanization; state of cure; conversion

INTRODUCTION

A conveyor belt is a fabric-reinforced elastomeric composite like tire, which is conventionally cured by the intermittent process.[1] In recent years, however, attempts have been made to use the continuous process as an alternative method.[2] This is because the latter has proved to have the advantage of being more economical and the capability of producing higher-quality products. Conveyor belts produced by the continuous process show only 2.5% growth in overall length in 900 h of loading, while, under identical conditions, the belts produced by the conventional method exhibit 2.5% growth in less than 200 h.

Optimization and controlling the production line of the conveyor belt continuous curing process needs a good knowledge of the temperature distribution within the layers. However, heterogeneity of the conveyor belt and the transient nature of the heating, combined with the complexity of the curing reaction, have made this process difficult to be analyzed by simple analytical methods. There have been only a few reports concerning this particular subject and existing reports are limited to a patent.[2] However, several works have been published on the curing process of other rubber systems like tire,[3,4] which can provide a reliable ground for analyzing the continuous curing process of conveyor belts.

THEORETICAL STUDY

The differential equation governing the transient three-dimensional heat conduction applicable to the rubber curing process has been defined[3,5] as

$$\frac{\partial}{\partial x}\left(\lambda\frac{\partial T}{\partial x}\right)+\frac{\partial}{\partial y}\left(\lambda\frac{\partial T}{\partial y}\right)+\frac{\partial}{\partial z}\left(\lambda\frac{\partial T}{\partial z}\right)+\frac{dQ}{dt}=\rho c_p\frac{\partial T}{\partial t} \quad (1)$$

where T is the temperature; Q, the heat of the curing reaction; C_p, the heat capacity; ρ, the density; and λ, the temperature-dependent thermal conductivity defined as $\lambda = a - bT$ (a and b are constants). The above equation can be solved by

Correspondence to: H. Nazockdast.

Journal of Applied Polymer Science, Vol. 77, 2448–2454 (2000)

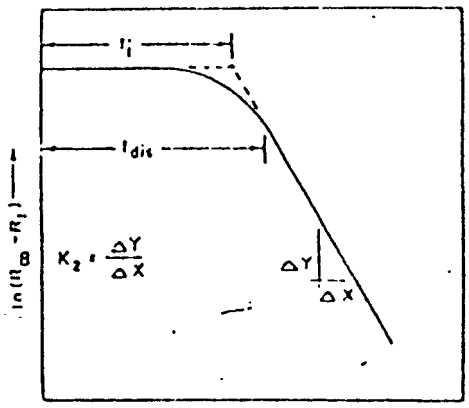

Figure 1 Determination of curing rate constant using the rheometry method.

the well-known implicit Crank Nichelson method for a given Q and λ.

The curing reaction of rubber compounds is not highly exothermic. However, due to the low thermal conductivity of the compounds, it can lead to an appreciable increase in temperature and, hence, an increase in the rate of the curing reaction. Considering the curing reaction as a first-order reaction, the overall rate of cure can be defined by a single expression with a constant activation energy as (see Fig. 1)

$$dQ/dt = K_0(Q_\infty - Q_t)\exp(-E/RT) \qquad (2)$$

where Q_t is the heat of the cure reaction up to time t, Q_∞ the total heat of curing, E the reaction activation energy, and K_0 is the reaction constant to be independent of temperature. E and K_0 can be evaluated by rheometry method[6] as described in Figure 1. The temperature distribution obtained for the conveyor belt can be utilized in a proper way to evaluate the extent of the curing reaction and the state of cure (SOC)[4] defined as

$$\mathrm{SOC} = \int_0^t \bar{K}^{(T-T_R)/10}dt \qquad (3)$$

where T is the temperature at time t; T_R, the reference temperature; and $\bar{K}$, the vulcanization temperature coefficient reported to be within the range of 1–1.9 for each of the layers.[4]

It is generally accepted that for most rubber compounds there are three periods during vulcanization, namely, the induction period, curing stage, and postcuring. During the induction period, no chemical reaction occurs. Thus, $dQ/dt = 0$ at $t \le t_0$, where t_0 is the induction time. It is noted that in eq. (3) the induction time, t_0, has not been taken into account and the curing reaction has been considered as a zero-order reaction. In the present work, we have treated these in a more realistic way by considering the curing reaction as a first-order reaction and taking into account the induction time. Thus, for the curing reaction defined as[7] $x = Q_t/Q_\infty$, the conversion may be defined as

$$X = 1 - \exp\int_{t_0}^{t} -Kdt \quad \text{at} \quad t > t_0 \qquad (4)$$

and

$$X = 0 \qquad \text{at} \qquad t \le t_0 \qquad (5)$$

The curing rate constant K and the induction time t_0, are considered as temperature dependent parameters expressed by Arrenius-type equation[8] as:

$$K = K_0\exp(-E/RT) \qquad (6)$$

$$t_0 = B\exp(-E_t/RT) \qquad (7)$$

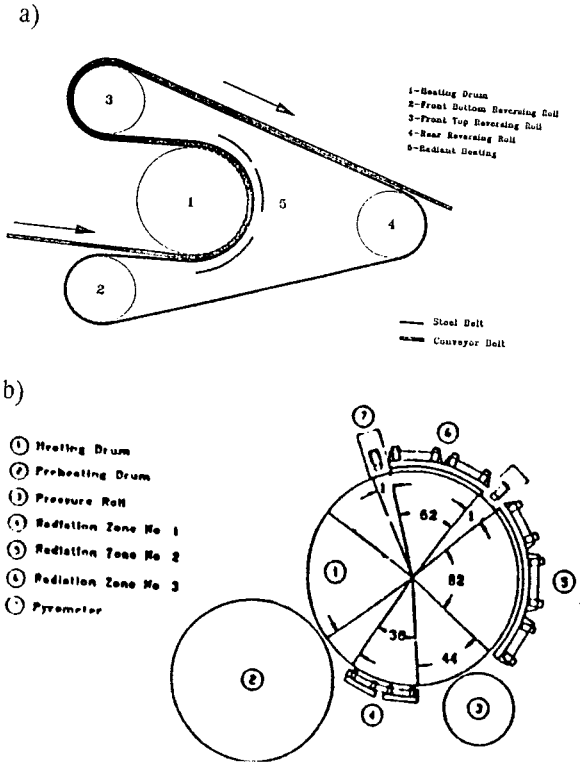

Figure 2 Schematic diagram of (a) continuous curing process and (b) Roto-Cure system.

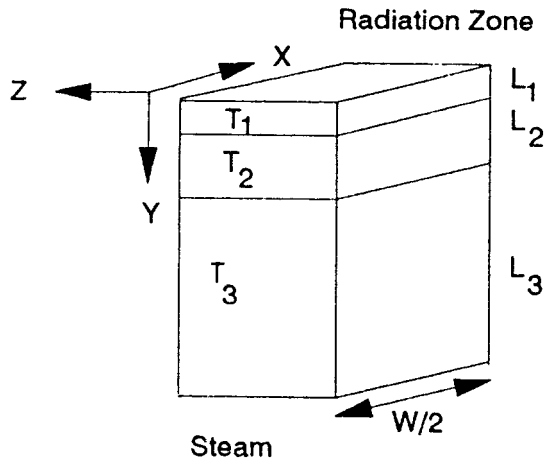

Figure 3 The moving element consisting of a steel belt. (layer 1), conveyor belt (layer 2), and heating drum shell (layer 3).

MATHEMATICAL MODELING

Conveyor belts are usually made of a few number of fabric plies joined together by interplies with top and bottom rubber covers. Schematic diagrams of the continuous curing process and corresponding Roto-Cure system[9] used in this investigation are shown in Figure 2.

The system shown in Figure 2 consists of a preheating drum, heating drum, and radiation heaters. The heating drum is divided into zones with angles as indicated. As the heating path of the process employed in the present work is in curved form, the cylindrical coordinate may be the most appropriate system for obtaining a required partial differential equation. However, since the aspect ratio (length/thickness) is high, the mathematical modeling can be established in a Cartesian coordinate system. For the same reason, the process can be considered as a two-dimensional system. Therefore, the governing equation will be

$$\frac{\partial^2 T}{\partial x^2} + \frac{\partial^2 T}{\partial^2 y} + \frac{dQ}{dt} = \frac{1}{\alpha}\frac{\partial T}{\partial^2 t} \tag{8}$$

where α is thermal diffusivity. Due to the dynamic nature of the system, the heat-transfer equation used for modeling was derived from the Lagrangian coordinate (moving element). To apply the proper boundary condition, the final condition of the moving element was used as the initial condition for the next time interval Δt. Figure 3 shows the moving element consisting of three layers. Layer 1 is the steel belt which is in contact with the bottom cover of the conveyor belt; layer 2, the conveyor belt, and layer 3, the heating drum shell.

Thus, the equations and boundary conditions for each layer of the element are as follows:

Layer (1):

$$\frac{\partial^2 T_1}{\partial x^2} + \frac{\partial^2 T_1}{\partial y^2} = \frac{1}{\alpha}\frac{\partial T_1}{\partial t} \tag{9}$$

$$T_1(x, y, 0) = T_1$$

$$k_1\frac{\partial T_1}{\partial y} = h_r A_1(T_1 - T_E) + h_c A_1(T_1 - T_\infty) \quad \text{at} \quad y = 0$$

$$k_1\frac{\partial T_1}{\partial y} = k_2\frac{\partial T_2}{\partial y} \quad \text{at} \quad y = L_1$$

$$-k_1\frac{\partial T_1}{\partial x} = h_x(T_1 - T_\infty) \quad \text{at} \quad x = w/2$$

$$\frac{\partial T_1}{\partial x} = 0 \quad \text{at} \quad x = 0$$

Layer (2):

$$\frac{\partial^2 T_2}{\partial x^2} + \frac{\partial^2 T_2}{\partial y^2} = \frac{dQ}{dt} + \frac{1}{\alpha}\frac{\partial T_2}{\partial t} \tag{10}$$

$$T_2(x, y, 0) = T_2$$

Table I Values of Induction Time, t_0, Measured as a Function of Temperature

	T (°C)						
	133	137	141	145	149	154	158
Parameter	t_0 (min)						
Cover	17	10.8	7.6	6.4	5.7	4.4	4
Carcass	13	10	9.0	6.7	5.2	4	3.8

Table II Calculated Values of Arrhenius Constants in Eqs. 6 and 7

Parameter	K_0 (s^{-1})	E (kcal, mol^{-1})	E_1/R	B
Cover	3.7×10^6	17.173	9602.906	7.5×10^{10}
Carcass	1.5×10^{10}	23.415	8919.341	3.7×10^{-9}

$$T_2 = T_1 \quad \text{at} \quad y = L_1$$

$$T_2 = T_3 \quad \text{at} \quad y = L_1 + L_2$$

$$-k_2\frac{\partial T_2}{\partial x} = h_x(T_2 - T_\infty) \quad \text{at} \quad x = w/2$$

$$\frac{\partial T_1}{\partial x} = 0 \quad \text{at} \quad x = 0$$

Layer (3):

$$\frac{\partial^2 T_3}{\partial x^2} + \frac{\partial^2 T_3}{\partial y^2} = \frac{1}{\alpha}\frac{\partial^2 T_3}{\partial t} \tag{11}$$

$$T_3(x, y, 0) = T_3$$

$$k_3\frac{\partial T_3}{\partial y} = k_2\frac{\partial T_2}{\partial y} \quad \text{at} \quad y = L_1 + L_2$$

$$k_3\frac{\partial T_3}{\partial y} = h_s(T_3 - T_\infty) \quad \text{at} \quad y = L_1 + L_2 + L_3$$

$$\frac{\partial T_3}{\partial x} = 0 \quad \text{at} \quad x = w/2$$

$$T_{\infty b} = T_{\text{Steam}}$$

In the above equations, k_1, k_2, and k_3 are the thermal conductivity of the layers; α, the thermal diffusivity and h_c, h_x, and h_b, convective heat-transfer coefficients corresponding to varying locations of the belt calculated according to ref. 10. A_1 is the area of layer 1 of the moving element subjected to the radiation zone; T_∞, the ambient temperature in each zone; $T_{\infty b}$, the steam temperature, and h_r, the radiation coefficient calculated according to following equation 11:

$$h_r = \frac{\sigma(T_E^2 + T_1^2)(T_E + T_1)}{\frac{A_1}{A_E}\frac{1 - \varepsilon_E}{\varepsilon_E} + \frac{1}{F_{1E}} + \frac{1 - \varepsilon_1}{\varepsilon_1}} \tag{12}$$

where F_{1E} is a view factor which can be calculated on the basis of the relation between the movement of the element against the heating zone[12] and ε is the emissivity.

The problem was solved by using a numerical method based on the implicit algorithm (Crank Nichelson). The final equations, after substituting the finite difference form in eqs. (9)–(11), are presented as follows:

at time $n + 1$:

$$F = T_{ij}^{n+1}(1 + N_1 + M_1) - \tfrac{1}{2}N_1T_{i+1j}^{n+1} - \tfrac{1}{2}N_1T_{i-1j}^{n+1} - \tfrac{1}{2}M_1T_{ij+1}^{n+1} - \tfrac{1}{2}M_1T_{ij-1}^{n+1} \tag{13}$$

at time n:

$$F = T_{ij}^{n}(1 - N_1 - M_1) + \tfrac{1}{2}N_1T_{i+1j}^{n} + \tfrac{1}{2}N_1T_{i-1j}^{n} + \tfrac{1}{2}M_1T_{ij+1}^{n} + \tfrac{1}{2}M_1T_{ij-1}^{n} \tag{14}$$

$$M_1 = \frac{\alpha\Delta t}{\Delta y^2} \quad N_1 = \frac{\alpha\Delta t}{\Delta x^2}$$

Table III Thermal Diffusivity, α, Heat of Vulcanization, Q, Conductivity, K, and Emissivity, ε, Evaluated for Steel Belt, Conveyor Belt, and Heating Drum Shell

Parameter	α (m^2/h)	Q (cal/g)	K (w/m K)	ε	Thickness L (mm)
Steel belt			17	5.45	$L_1 = 2$
Cover	3.12×10^{-4}	−7	0.35–0.00057 T °C		$L_2 = 10$
Carcass	3.42×10^{-4}	−8			
Heating drum shell			45		$L_3 = 40$

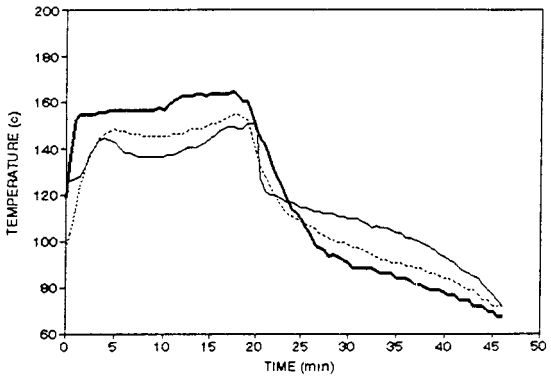

Figure 4 Temperature profile measured for three layers within the conveyor belt; (—) top cover (. . .) between top cover and carcass (—) bottom cover contacting steel belt. Belt thickness, 10 mm, and curing time, 19 min.

and

$$\left(\frac{dQ}{dt}\right)_{i+1} \Delta t = Q_{i+1} - Q_i = (Q_\infty - Q_t)K_0 \exp(-E/RT)\Delta T$$

$$Q_0 = 0 \quad Q_i = \sum_{j=0}^{i}\left(\frac{dQ}{dt}\right)_j \Delta t$$

EXPERIMENTAL

The curing of conveyor belt samples was carried out in the same Roto-Cure system as that described in Figure 2 for the modeling. The experiments were performed on belts of 10 and 6 mm thickness but with the same composition. The temperatures of the layers within the conveyor belt and of the top and bottom surfaces of the rotary press were measured using Cu—Ni thermocouples placed inside the layers while moving with the belt, covering the entire cure path. To avoid damaging the steel-belt surface, the thermocouple wires were led through narrow grooves curved on the outer surface of the bottom cover.

The curing reaction constant (K) and the induction time (t_0) were measured as a function of the temperature using the rheometry technique according to ref. 6. The values obtained for K and t_0 were used in eqs. (6) and (7) in order to calculate K_0, E/RT, B, and E_1/RT. The calculated results are given in Tables I and II. Thermophysical parameters of the steel belt, drum shell, and the conveyor belt are given in Table III.

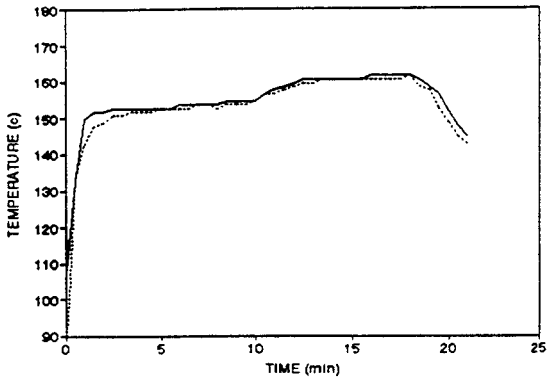

Figure 6 Temperature distribution measured along the width (150 cm) of the top cover of the conveyor belt: (. . .) 35 cm, and (—) 80 cm.

RESULTS AND DISCUSSION

Results of the temperature measurements are illustrated in Figures 4–6. Figure 4 demonstrates the temperature profiles of the three layers

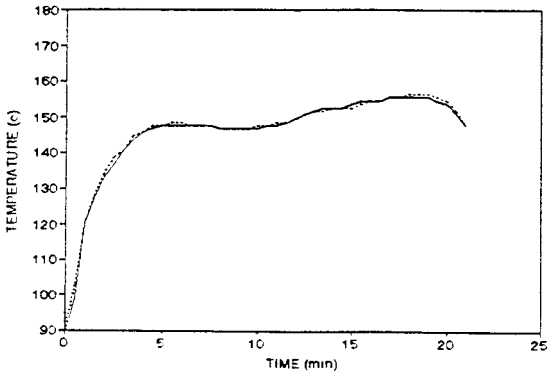

Figure 5 Temperature profile of a layer between the top cover and the carcass obtained from two separate experiments, indicating excellent reproducibility for the temperature measurements.

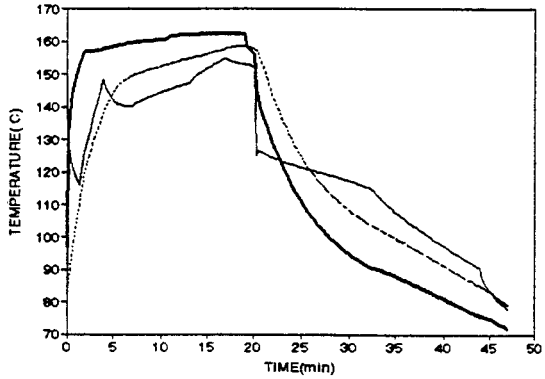

Figure 7 Theoretically predicted temperature profile of various layers within the belt; (—), top cover (. . .) between top cover and carcass, (—), bottom cover contacting steel belt. Belt thickness, 10 mm; curing time, 19 min.

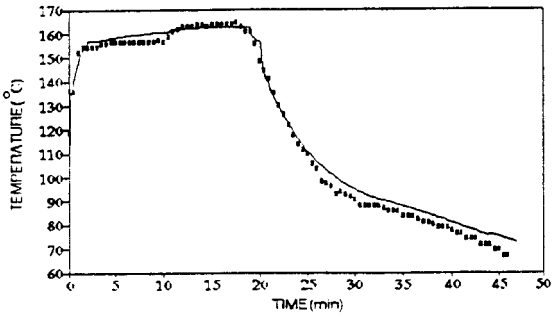

Figure 8 Temperature profile of the top cover of the belt. (. . .) Experimental, (—) theoretical. Thickness, 10 mm; curing time, 19 min.

within the conveyor belt during the curing and postcuring processes. As can be seen, various layers within the belt experience different temperature distributions during the curing process. The temperature of all layers decrease as the belt leaves the heating drum and subsequently approaches approximately the same temperature ($\approx$ 115°C). From this point, however, they follow different trends of reduction in their temperature. These later results can be attributed to the heat of reaction which takes place during the postcuring process. This is due to the presence of the steel belt which reduces the rate of heat transfer, hence providing more opportunity for the curing reaction to have taken placed during the postcuring process. Thus, as shown in Figure 4, the highest amount of postcuring takes place in the outer surface of the bottom cover, and the lowest, in the uppermost surface of the top cover.

Figure 5 shows two temperature profiles obtained from two separate experiments performed under identical conditions for a layer between the top cover and the carcass. These results indicate excellent reproducibility for the temperature measurements made in the present investigation. Figure 6 demonstrates that there is no appreciable variation in the temperature across the width

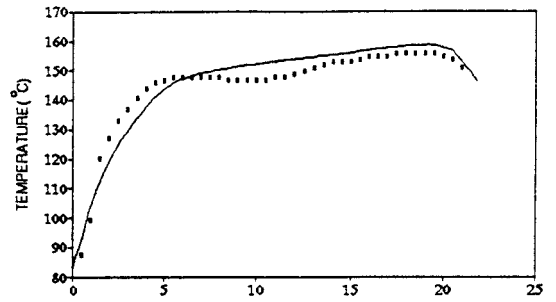

Figure 9 Temperature profile of a layer between the top cover and carcass: (. . .) experimental; (—) theoretical.

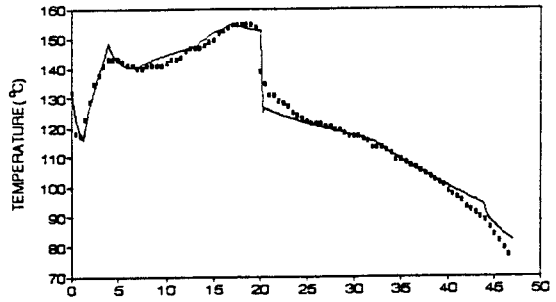

Figure 10 Temperature profile of the layer contacting the steel belt: (. . .) experimental; (—) theoretical.

of the belt. The results of the temperature distribution predicted by the mathematical model for various parts of the conveyor belt are illustrated in Figures 7–10.

Comparing these results with those shown in Figure 4 reveal that there is good agreement between the theoretical and experimental results. Having justified the reliability of the mathematical model, it was employed to provide more insight into the curing process, in terms of the SOC and the degree of conversion of various layers within the conveyor belts. Typical results predicted for the SOC and the degree of conversion are shown in Figures 11–13.

The results shown in Figure 11 demonstrate that for the belt with 10 mm thickness and cured in 19 min the SOC of each layer is strongly influenced by the temperature distribution experienced by them during the curing process. As can be seen, there is an appreciable difference between the SOC of the top and bottom covers of the

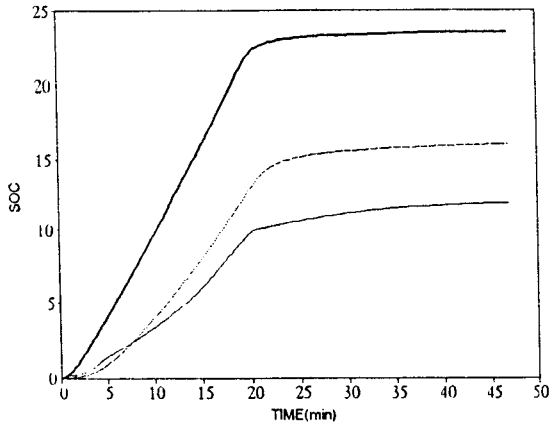

Figure 11 Variation of SOC as a function of curing time for three layers within the belt with 10 mm thickness and cured for 19 min. (—) Top cover; (. . .) between top cover and carcass, (—) bottom cover contacting steel belt.

belt, which nearly persists throughout the curing and postcuring periods. The results presented in Figure 12 suggest that the difference between the SOC of the layers within the products can be reduced, but not necessarily vanish, when conveyor belts with 6 mm thickness are used.

The results presented in Figure 13 show that the variation in the degree of conversion of the layers during the curing process follow the same trends as those of the SOC. However, comparing these results with the experimental results shown in Figure 4 reveals that the degree of conversion, as determined in this work, is a more appropriate criterion than is the SOC for predicting the influence of the postcuring process.

According to Prentice and Williams,[4] a minimum of 8 equiv min (SOC $\approx$ 8 min) is required to obtain a soft cure. The optimal properties are developed in 16–35 equiv min and some deterioration of the properties occur above 50 equiv min. As shown in Figure 8 for the conveyor belt with 10 mm thickness and cured for 19 min, the SOC predicted for the bottom cover is about 11, which may be within the acceptable range but not optimum. However, as can be seen in Figure 9, the SOC predicted for the conveyor belt with 6 mm thickness and cured for 15 min are within the optimum range. These results reveal that the above-described mathematical model has the capability of being utilized for optimization of the present conveyor belt continuous curing process. This part of the work was carried out in our laboratory and results are to be published in the early future.

CONCLUSIONS

The results predicted by the mathematical model developed in the present work were found to be in good agreement with the experimental results, therefore justifying the capability of the model for simulation of the conveyor belt continuous curing process. The model was also found to be capable of generating valuable information on the SOC and/or the degree of conversion, which can, in turn, be utilized for optimization of the curing process. Finally, it was found that the postcuring process can play an important role in the overall curing of the products.

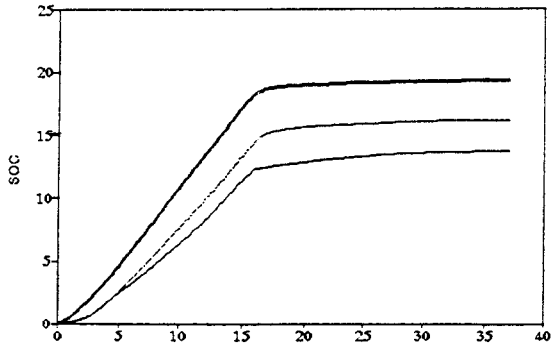

Figure 12 As in Figure 11 for the belt with 6 mm thickness and cured in 15 min.

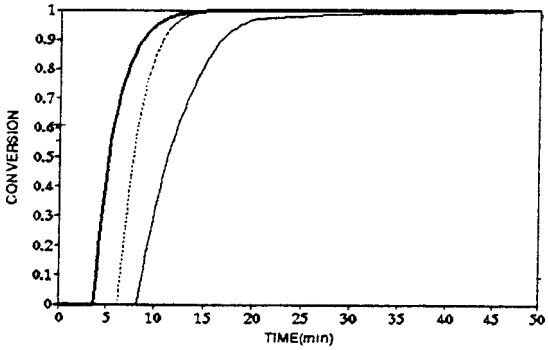

Figure 13 Degree of conversion as a function of curing time for three layers within the belt with 10 mm thickness and cured for 19 mm. (—) Top cover; (. . .) between top cover and carcass; (—) bottom cover contacting steel belt.

REFERENCES

1. Lepetov, V. A.; Fogel, V. O.; Tomchin, L. B.; Krainova, N. A. Sov Rubb Technol 1962, 27–29.
2. Goodyear Tire & Rubber Company U.S. Patent 982 377, 1962.
3. Accetta, A.; Gangnet, G.; Vergnaud, J. M.; Vincent, L. In 3rd International Conference on Computers and Chemical Engineering, Paris, 1983.
4. Prentic, G. A.; Williams, M. C. Rubb Chem Technol 1980, 53, 1023.
5. Khouider, A.; Rochette, J. B.; Vergnaud, J. M. Thermochim Acta 1985, 89, 81–92.
6. Coran, A. Y. Rubb Chem Technol 1984, 37, 689.
7. Isayev, A. I.; Deng, J. S. Rubb Chem Technol 1988, 61, 340.
8. Claxton, W. E.; Liska, J. W. Rubb Age 1964, 9(5), 237.
9. Berstroff, H. Technical Documents AUMA 15 S $\times$1500, Machine No. 90-1-Ao. 6733–47184.
10. Holman, J. P. Heat Transfer; McGraw Hill: New York, 1981.
11. Incropera, F. P.; Dewit, D. P. Fundamentals of Heat and Mass Transfer; Wiley: New York, 1981, 1985; p 646.
12. Sparrow, E. M.; Ces, R. D. Radiation Heat Transfer; Wudsworth: Belmont, CA, 1970.